CIGS Solar Cell on Flexible Stainless Steel Substrate Fabricated by Sputtering Method: Simulation and Experimental Results

Rui Zhang, Dennis R. Hollars[1] and Jerzy Kanicki[*]

Dept. of Electrical Engineering and Computer Science, University of Michigan, Ann Arbor, MI 48109, U.S.A.
Phone: +1-734-916-0972 Fax: +1-734-615-2843 [*]E-mail: kanicki@eecs.umich.edu
[1]NuvoSun, San Jose, CA 95131, U.S.A.

We reported on opto-electronic properties of the Cu(InGa)Se_2 (CIGS) solar cell fabricated by sputtering method on stainless steel substrate having external efficiency of ~13.0%. Experimental data indicates that the quantum efficiency (QE) has a high response for long wavelength light. Current density (J) - voltage (V) measurements under illumination resulted in short circuit current density of 32.08 mA/cm^2 and open circuit voltage of 0.55 V. We have also performed modeling of this device establishing that both experimental and calculated data are consistent with each other.

1. Introduction

Flexible $Cu(In_{1-x}Ga_x)Se_2$ (CIGS) solar cells are very attractive device that can be used in many applications requiring flexible or/and conformal substrates. Several groups have reported in the past few years on development of CIGS solar cell on flexible substrates. Kim and Ahn et al.[1)] reported a flexible CIGS solar cell on stainless steel substrate by co-evaporation process with efficiency of ~10.57%. Herrman and Kessler et al.[2)] investigated barrier layers for flexible CIGS thin-film solar cells on metal foils. The device fabricated on titanium foil achieved external efficiency of about 13%. Hashimoto and Negami et al. showed improved performance of CIGS solar cell on stainless steel by adding Na to the CIGS film; they achieved efficiency on the order of 17%. [3)] In this work, we fabricated a CIGS solar cell on flexible stainless steel substrate by sputtering. We measured opto-electronic properties of such device. We also did modeling of the solar cells structure. Finally we compared the experimental and simulated results.

2. Modeling and Experimental

Device Simulation

We performed modeling of Al:ZnO/i-ZnO/CdS/Cu(InGa)Se_2 (CIGS)/Mo solar cell using software APSYS. The APSYS simulator is a general purpose 2D/3D finite element analysis and modeling software for semiconductor device. [4)] All simulations are done under an AM1.5 sunlight spectrum. Series resistance and shunt resistance obtained from measured current density (J) – voltage (V) curves are included in our simulation. The set of parameters needed for electrical and optical modeling was obtained from experimental data, form the literature and form precious work by others. Typical parameter set is shown in Table 1.

Table 1. Parameters set used for the modeling of CIGS solar cell

Parameters and Symbol	Unit	CIGS	CdS	Al:ZnO
dielectric constant ϵ_r	-	13.6	8.9	8.5
band gap E_g	[eV]	1.15	2.42	3.3
electron affinity x_e	[eV]	4.5	4.8	4.7
electron mobility μ_n	[$cm^2V^{-1}s^{-1}$]	60	35	100
hole mobility μ_h	[$cm^2V^{-1}s^{-1}$]	10	16	31
electron lifetime τ_n	[s]	10^{-8}	10^{-9}	10^{-8}
hole lifetime τ_p	[s]	10^{-8}	10^{-9}	10^{-8}
real index n_{real}	-	2.6	2.4	2.0
absorption α_0	[cm^{-1}]	2.8×10^{-5}	3.4×10^{-4}	-

Device Fabrication

Solar cells Al:ZnO/i-ZnO/CdS/CIGS/Mo/Cr/stainless steel investigated in this work was fabricated as follow. [5)] The 2' wide mil thick stainless steel substrates were first cleaned by ion etch prior to the deposition of a Cr barrier layer, followed by the deposition of Mo back electrode. Cu, In and Ga were deposited by rotary magnetron sputtering on to a stainless steel substrate in the presence of a flux of Se. Substrate temperature was 485℃ ±10℃. During deposition of CIGS Na was provided through sputtering from a NaF target. Then CdS was deposited by chemical bath deposition (CBD). Intrinsic ZnO and Al:ZnO were sputtered as follow up step. Al-doped Zn oxide is used as transparent electrode. We mechanically scribed different areas of the device studied in this work. No antireflection (AR) coating was used. The device opto-electronic properties such as J-V characteristics were

measured under a simulated AM1.5 solar spectrum with an intensity of 100mW/cm^2. Quantum efficiency versus wavelength curve was also measured. The device performances were evaluated under various light intensities.

3. Results and Discussion

The calculated band diagram of the investigated device under open circuit voltage (Voc) is shown in Figure 1. From left to right are back contact Mo (0.5 um), CIGS (2 um), buffer CdS (0.05 um) and window i-ZnO (0.25 um), and transparent electrode Al:ZnO (0.25 um) layer, respectively.

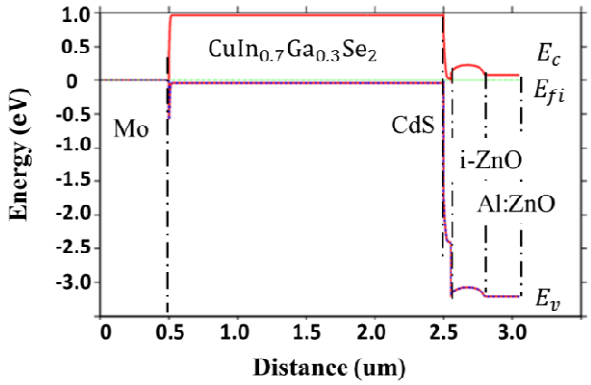

Fig. 1. Calculated band diagram at open circuit voltage of the CIGS photovoltaic device investigated in this work.

The optical absorption distribution across the device is also shown in Figure 2. The calculated relative energy density is showing optical absorption of different layer under AM 1.5 illumination. As expected the absorbed optical energy decreases along light incident path. Specially, ZnO and CdS layer absorbed considerable amount of light, but any electron-hole pairs generated in these regions cannot be collected. This will cause absorption loss. Reducing the thickness of these layers can minimize these losses. [6)]

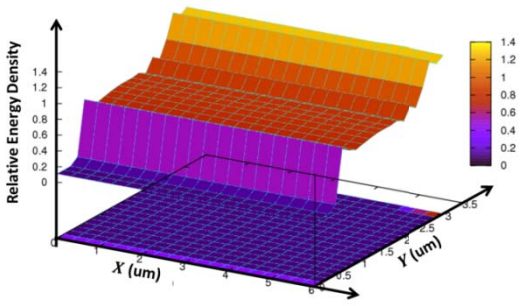

Fig. 2. Relative energy density showing optical absorption across solar cell.

Figure 3 shows the simulated J-V curves for CIGS solar cell without series resistance (Rs) and shunt resistance (Rsh), and with Rs=2.91 Ωcm^2, Rsh=700 Ωcm^2, respectively. Jsc and Voc are extracted from the intercepts on Y and X-axis respectively. The maximum power point (P_{max}) is found by tracing the point which has the maximum $J \cdot V$. The current density and voltage in this point are defined as J_{MP} and V_{MP}. Fill factor (FF) and efficiency (η) are then calculated by:

$$FF = \frac{P_{max}}{V_{oc} \cdot J_{sc}} = \frac{V_{MP} \cdot J_{MP}}{V_{oc} \cdot J_{sc}} \quad (1)$$

$$\eta = \frac{P_{max}}{P_{inc}} \times 100\% = \frac{V_{oc} \cdot J_{sc} \cdot FF}{P_{inc}} \times 100\% \quad (2)$$

In this work, solar cell without Rs and Rsh has following performance: η=14.3%, Voc=0.58V, Jsc=30.0mA/cm^2, FF=0.84 while device with the Rs and Rsh has performance as follow: η=12.1%, Voc=0.58V, Jsc=29.4mA/cm^2, FF=0.71. The Rs and Rsh is responsible for reduction of FF and solar cell external efficiency.

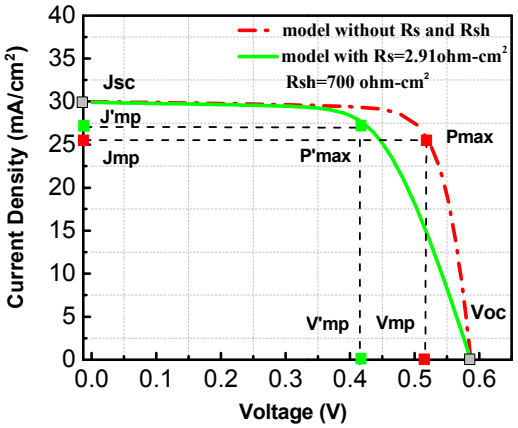

Fig. 3. Calculated J - V curve of CIGS solar cell under AM1.5 illumination.

Devices with different sizes were fabricated and measured. The experimental J-V curves for solar cell with 0.043cm^2 device area in dark and under illumination are shown in Figure 4, respectively. From the J-V curve in dark, we can extract the reverse saturation current density (Jo) from the intercept on Y-axis. From the slope of J-V characteristic under illumination, as shown in Figure 4, we extract series resistance (Rs) and shunt resistance (Rsh) as follow: [7-8)]

$$R_s = \frac{dV}{dJ}\Big|_{V=V_{oc}} = \frac{\Delta V_{oc}}{\Delta J_{oc}} \quad (3) \quad \text{and} \quad R_{sh} = \frac{dV}{dJ}\Big|_{J=J_{sc}} = \frac{\Delta V_{sc}}{\Delta J_{sc}} \quad (4)$$

The performance of the fabricated photovoltaic device is

η =11.3%, Voc=0.52V, Jsc=32.15mA/cm^2, FF=0.67, Rs= 2.91 Ω cm^2, Rsh=773 Ω cm^2 and Jo=3 × 10^{-4}mA/cm^2. The experimental result agrees well with the calculated results (η=12.1%, Voc=0.58V, Jsc=29.4mA/cm^2, FF=0.71) without doing any extensive optimization of the device parameters used in this calculation. The similarity between both results indicates that simulation of CIGS is accurate and can be used in optimization of flexible CIGS photovoltaic cells opto-electronic properties.

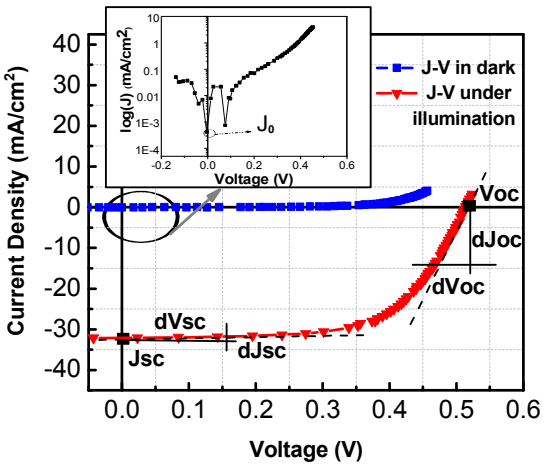

Fig. 4. Experimental J-V curve of our CIGS solar cell measured under AM 1.5 illumnation..

Table 2 shows performance of the CIGS solar cells with different device areas. All devices have similar Jsc and Voc. However, larger area device shows a lower FF and external efficiency. With the increasing of device area, Rs increases while Rsh is reduced. Both these parameters will affect device FF and solar cell efficiencies.

Table 2. Performance of CIGS solar cells having different cell areas.

Area (cm^2)	Rs (Ωcm^2)	Rsh (Ωcm^2)	FF	Jsc (mA/cm^2)	Voc (V)	η (%)
0.03	1.16	896	0.73	32.08	0.55	13.0
0.04	2.91	773	0.67	32.15	0.52	11.3
0.16	7.45	628	0.46	32.06	0.51	7.52
0.25	9.50	501	0.38	30.01	0.49	5.59

The fill factors variation with the series resistance is shown in Figure 5. Hence these results indicate that for a large area solar cell, reducing the series resistance is critical to achieve high efficiency. Therefore, as expected, for larger area devices metal grids must be used to maintain higher device efficiency.

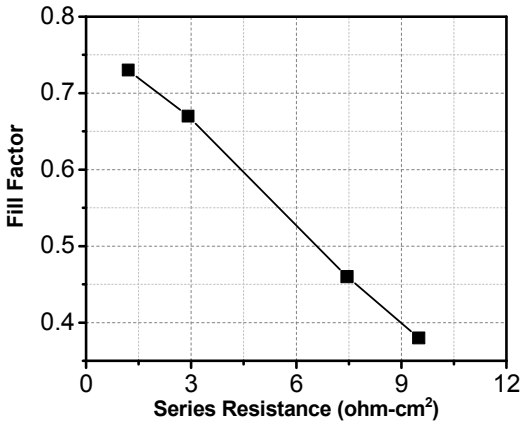

Fig. 5. The variation of fill factor versus series resistance of the CIGS solar cell.

Figure 6 shows variation of external quantum efficiency (QE) versus wavelength (λ) for our photovoltaic cell. The device QE is close to 90% at the maximum and remains no less than 40% QE up to 1200nm. From the definition of external quantum efficiency:

$$QE = \frac{J_{sc}/q}{P_{inc}/h\nu} \qquad (5)$$

where $\nu = \frac{c}{\lambda}$, h is Planck constant ($6.63 \times 10^{-34} J \cdot s$), $q = 1.6 \times 10^{-19}$C and P_{inc} is incident light power density (mW·cm^{-2}), we can derive the expression of short circuit density for a given wavelength incident light:

$$J_{sc}(\lambda) = \frac{q\lambda}{hc} \cdot P_{inc}(\lambda) \cdot QE(\lambda) \qquad (6)$$

$$P_{inc}(\lambda) = f(\lambda)d\lambda \qquad (7)$$

where $f(\lambda)$ is light spectrum intensity (mW·cm^{-2}·nm^{-1}). Then total short circuit current density can be obtained by integrating all $J_{sc}(\lambda)$ over all incident light spectrum:

$$J_{sc} = \int J_{sc}(\lambda) = \int \frac{q \cdot \lambda}{hc} f(\lambda) QE(\lambda) d\lambda \qquad (8)$$

In our experiment, the incident light spectrum is AM1.5 sunlight spectrum and P_{inc}=$\int f(\lambda)d\lambda$=100mW·cm^{-2}. The value of total short circuit current density over all sunlight spectrum of the cell is 32.15mA/cm^2. Plot in Figure 6 also shows that QE drops very quickly from 520nm (corresponding to CdS band gap of 2.42eV) to 300nm. Light absorption in CdS layer is responsible for this decrease, since it is commonly observed that electron-hole pairs generated in the CdS cannot be collected. Therefore, reduction of

the thickness of CdS is expected to reduce this absorption loss and increase device output current.

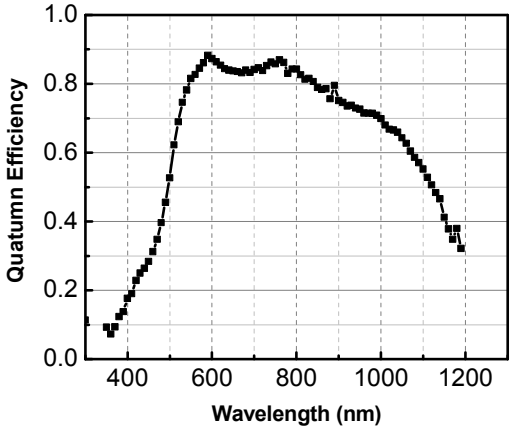

Fig. 6. Measured QE - λ curve of our CIGS solar cell device.

Figure 7 shows changes of Jsc and Voc under different light intensities (X). Under a given light intensity, the incident light power density can be expressed as:

$$P_{inc}(X)=X \cdot P_{inc} \qquad (9)$$

Then Jsc under a given light intensity can be expressed as a function of X, by applying eq. (9) into eq. (8):

$$J_{sc}(X) = \int \frac{q\lambda}{hc}(X \cdot P_{inc}(\lambda)) \cdot QE(\lambda) = J_{sc} \cdot X \qquad (10)$$

where J_{sc} is the short circuit density under 100% of AM1.5 illumination, which is equal to 32.15 mA/cm^2. The red line represents fitting to experimental data using eq. (10).

And for Voc, we have general equation as follow: [6]

$$V_{oc} = \frac{nk_BT}{q} In\left(\frac{J_{sc}}{J_0}+1\right) \qquad (11)$$

By substituting J_{sc} with $J_{sc}(X)$ into eq. (11), we can get Voc under a given light intensity as a function of X:

$$V_{oc} = \frac{nk_BT}{q} In\left(X \cdot \frac{J_{sc}}{J_0}+1\right) \qquad (12)$$

where k_B is Boltzmann constant (1.38×10^{-23}J·K^{-1}), T=300K, J_0= 3×10^{-4}mA/cm^2, n=1.7. The calculated blue curve based on eq. (12) can fit well experiment data. This result indicates that a fluctuation of light intensity may cause a large change of current output in a series connected solar cell module while its voltage output is relatively stable.

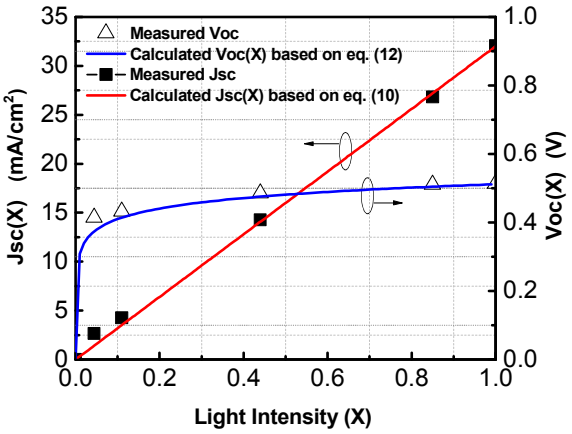

Fig. 7. Jsc and Voc as functions of light intensity X for CIGS solar cell.

4. Conclusions

We measured opto-electronic properties of flexible CIGS solar cell on stainless steel substrate fabricated by sputtering method. We have shown that simulated results are consistent with the experimental data. Therefore, simulation tool used in this work can be very useful in the design and optimization of the CIGS solar cells performance before its fabrication. This will allow very fast and cost effective design of the CIGS solar cells with the best properties. We have shown that it is possible to fabricate solar cells on flexible stainless steel substrate by sputtering method with acceptable opto-electronic properties and external efficiency.

Acknowledgements

The authors gratefully acknowledge Dr. Yan, Baojie of Uni-solar for his assistance with the measurements. Dr. Y. G. Xiao of Crosslight is also acknowledged for his support with the APSYS software.

References

1) Min Sik Kim et al., 2007, Solid State Phenomena, 124-126, pp. 73-76

2) D. Herrmann et al. Mat. Res. Soc. Symp. Proc. Vol. 763 (2003) B6.10.1

3) Hashimoto, Y. et al. Proceedings of 3rd World Conference on Photovoltaic Energy Conversion 2003, pp. 574-577, ISBN 4-9901816-0-3

4) Y. G. Xiao et al. PVSC 2010 35th IEEE 001990-001994 ISSN: 0160-8371

5) D.R. Hollars et al. Mater. Res. Soc. Symp. Proc Vol.865 (2005) F14.34.1

6) W. N. Shafarman, S. Siebentritt, L. Stolt et al. Handbook of Photovoltaic Science and Engineering, second edition (2011) ISBN: 978-0-470-72169-8

7) D. Sera et al. IECON' 09 35th Annual Conference of IEEE, pp. 800-805.

8) C. Zhang, J. Zhang, Y. Hao et al. J. Appl. Phys. 110, 064504 (2011)